

# Excited State Dynamics of Methyl Viologen. Ultrafast Photoreduction in Methanol and Fluorescence in Acetonitrile

Jorge Peon, Xin Tan, J. David Hoerner, Chungeng Xia, Yin Fei Luk, and Bern Kohler\*

Department of Chemistry, The Ohio State University, 100 W. 18<sup>th</sup> Ave., Columbus, Ohio 43210, U.S.A.

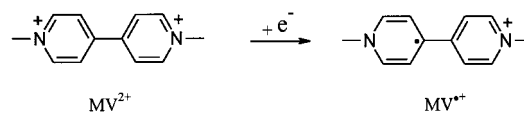
Received: December 31, 2000; In Final Form: March 30, 2001

The photophysical and photochemical deactivation pathways of electronically excited methyl viologen (1,1'-dimethyl-4,4'-bipyridinium,  $MV^{2+}$ ) were studied in several polar solvents at room temperature using a variety of ultrafast time-resolved and steady-state spectroscopic techniques. The results highlight the very strong electron accepting character of the lowest singlet excited state of  $MV^{2+}$ . Transient absorption was measured between 270 and 740 nm as a function of delay time after excitation of the strong  $\pi-\pi^*$  transition of  $MV^{2+}$  by a 150 fs, 265 nm pump pulse. In methanol, the radical cation of methyl viologen ( $MV^{\bullet+}$ ) appeared within our time resolution, indicating that forward electron transfer from a nearby donor quenches electronically excited  $MV^{2+}$  in  $< 180$  fs. Identical dynamics within experimental uncertainty were observed for the chloride salt of  $MV^{2+}$  and for the salt prepared with tetrafluoroborate counterions. This latter "superhalide" ion has a condensed-phase detachment threshold that is too high to permit oxidation by the excited state of  $MV^{2+}$ . Thus, electron transfer does not take place within an associated  $MV^{2+}$ -counterion complex in methanol but results instead from oxidation of a solvent molecule. Photoreduction of  $MV^{2+}$  in methanol is a novel example of ultrafast electron-transfer quenching of a photoexcited acceptor in an electron-donor solvent. This is the first demonstration that a hydrogen-bonding solvent can serve as the electron donor in an ultrafast intermolecular ET reaction. Decay of the initial  $MV^{\bullet+}$  population and simultaneous recovery of ground-state  $MV^{2+}$  with a characteristic time constant of  $430 \pm 40$  fs were observed immediately after the pump pulse and assigned to back electron transfer in the geminate radical pair. Despite the high rate of back electron transfer, a significant fraction of the initial radical pairs avoid recombination, and a finite yield ( $\sim 12\%$ ) of  $MV^{\bullet+}$  ions is observed at delay times  $> 2$  ps. There was no evidence of photoreduction when the solvent was acetonitrile or water. Both of these solvents have high gas-phase ionization potentials that prevent oxidation by excited  $MV^{2+}$ . The transient absorption signals indicate, however, that very different excited-state decay channels exist in these two solvents. In aqueous solution, an unknown nonradiative decay process causes decay of excited  $MV^{2+}$  with a time constant of 3.1 ps in  $H_2O$  and 5.3 ps in  $D_2O$ . In acetonitrile, on the other hand, the transient absorption decays hundreds of times slower and fluorescence is observed. This is the first report of an efficient radiative decay pathway for  $MV^{2+}$  in fluid solution. The excited-state absorption spectrum ( $S_1 \rightarrow S_N$  spectrum) of  $MV^{2+}$  was measured in acetonitrile and the fluorescence was characterized by time-correlated single-photon counting and steady-state measurements. The fluorescence quantum yield is  $0.03 \pm 0.01$  and the lifetime in acetonitrile at room temperature is  $1.00 \pm 0.04$  ns. The fluorescence is efficiently quenched by electron transfer from added quenchers with gas-phase ionization potentials lower than about 10.8 eV. Using the measured emission spectrum, the excited-state reduction potential is determined to be  $E^\circ(MV^{2+*}/MV^{\bullet+}) = 3.65$  V, confirming the highly oxidizing character of this photoexcited dication.

## Introduction

Methyl viologen (1,1'-dimethyl-4,4'-bipyridinium,  $MV^{2+}$  in Scheme 1) has attracted a great deal of study by a diverse group of chemists due to its wide-ranging applications.<sup>1</sup> The dichloride salt (trade name "paraquat") is a commercial herbicide that has been widely used for weed control.  $MV^{2+}$  has been investigated for solar energy conversion.<sup>2–5</sup> With a suitable catalyst  $MV^{2+}$  can produce hydrogen from water using visible light.<sup>5</sup> Because it is an organic dication it adsorbs strongly to negatively charged assemblies such as zeolites,<sup>3</sup> the sugar–phosphate backbone of DNA,<sup>6</sup> and silica gel.<sup>7</sup>  $MV^{2+}$  and its derivatives bind strongly to DNA and have been studied as potential photocleaving agents.<sup>8,9</sup> Photodamage in DNA has been studied by photo-

## SCHEME 1



induced electron transfer (ET) from an intercalated donor to externally bound  $MV^{2+}$ .<sup>10</sup> It has also been used to study ET in zeolites.<sup>3,11–14</sup>

These diverse applications are made possible by the strong electron accepting character of  $MV^{2+}$  and the stability of the radical cation ( $MV^{\bullet+}$  in Scheme 1) that is produced by one-electron reduction. The absorption spectrum of  $MV^{\bullet+}$  is characterized by two strong transitions, one in the near UV and one in the red ( $\lambda_{\max} = 396$  nm, and 606 nm in  $H_2O$ ,<sup>15</sup> see Figure 2). The violet color due to the latter transition is the reason that

\* To whom correspondence should be addressed. E-mail: kohler@chemistry.ohio-state.edu.

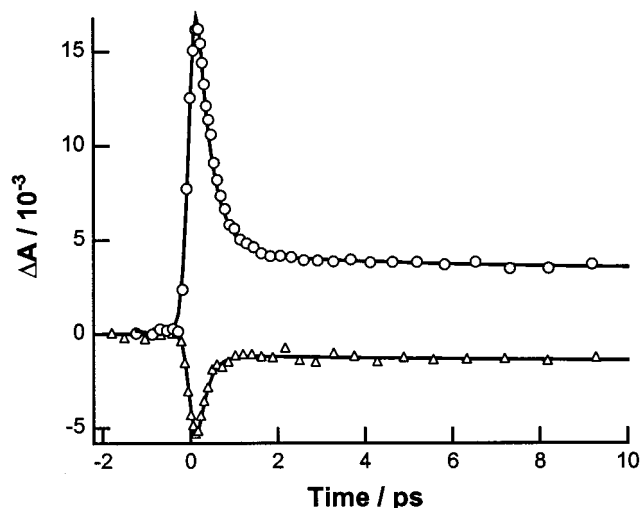


**Figure 1.** Transient absorption at 600 nm (circles) and at 270 nm (triangles) following photoexcitation of a 2.3 mM solution of the tetrafluoroborate salt of methyl viologen in methanol by a 150 fs, 265 nm pump pulse. The solid curves are from a global nonlinear least-squares fit (see text for details) to the data shown here plus additional transients at probe wavelengths between 270 and 700 nm.

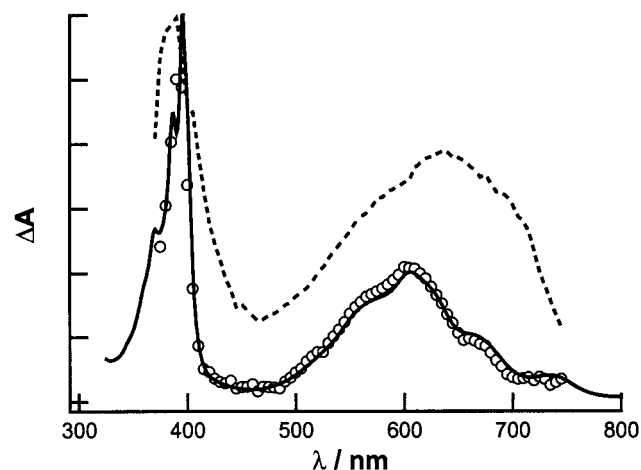


**Figure 2.** Transient absorption spectra recorded 2 ps after a 265 nm pump pulse for solutions of  $MV^{2+}(Cl^-)_2$  in methanol (open circles) and for  $MV^{2+}(PF_6^-)_2$  in acetonitrile (dashed curve). Both spectra have been corrected for group-delay dispersion ("chirp") and scaled to have the same maximum amplitude. The solid curve shows the steady-state absorption spectrum of the methyl viologen radical cation ( $MV^{\bullet+}$ ) generated by chemical reduction over Zn dust in deaerated  $H_2O$ . This spectrum has been scaled for comparison.

this and other dialkylated bipyridinium compounds are known as "viologens".  $MV^{\bullet+}$  is stable for many hours in room-temperature solution in the absence of oxygen,<sup>16</sup> and its absorption spectrum is insensitive to pH between pH 0–7.<sup>17</sup> These properties and the ease of spectroscopic detection of  $MV^{\bullet+}$  in the visible spectral region have made  $MV^{2+}$  a versatile redox indicator. In addition, it has been used to study fundamental issues in photoinduced electron transfer.<sup>18,19</sup>

In most of these applications electron transfer occurs to the electronic ground state of  $MV^{2+}$ . The favorable reduction potential of this state,  $E^\circ(MV^{2+}/MV^{\bullet+}) = -0.45$  V vs the normal hydrogen electrode (NHE),<sup>20</sup> is a measure of its good electron-accepting character. Much less is known about the higher-lying electronic states of  $MV^{2+}$ . Since electron accepting ability is strongly enhanced by electronic excitation,<sup>21,22</sup> ET should be even more favorable for the lowest excited singlet state. Indeed, Ledwith and co-workers reported a little over 30

years ago that photoexcitation of  $MV^{2+}$  in aqueous alcohol solution by ultraviolet (UV) light leads to the formation of  $MV^{\bullet+}$  and aldehydes.<sup>23,24</sup> Photoreduction was also observed in zeolites,<sup>12,25</sup> and several authors have commented on the strongly oxidizing character of electronically excited bipyridinium salts.<sup>7,26–28</sup>

Despite previous investigation by laser flash photolysis,<sup>29–32</sup> the elementary steps underlying the deactivation of excited  $MV^{2+}$  have remained unclear. Rodgers studied the photoreduction of  $MV^{2+}$  in neat methanol using nanosecond laser flash photolysis.<sup>29</sup> A significant amount of  $MV^{\bullet+}$  was generated faster than the experimental time resolution of 10 ns. Ebbesen et al. studied optically excited  $MV^{2+}$  under conditions that strongly favored association between this species and its counterions.<sup>30–32</sup> They showed that ET occurs in a complex between  $MV^{2+}$  and one or more chloride counterions faster than their experimental time resolution of approximately 30 ps. Because of their limited time resolution, they were unable to observe the ET dynamics directly. Furthermore, their work does not provide any information about free  $MV^{2+}$  ions in solution. We therefore undertook a systematic study of the excited-state dynamics of  $MV^{2+}$  using femtosecond pump–probe spectroscopy. This report emphasizes the dynamics of the free ion in several polar solvents in the absence of association with counterions. We show that in neat methanol, the lowest singlet excited state of  $MV^{2+}$  is quenched by ultrafast electron transfer from a solvent molecule. The measured first-order rates of forward and back ET are greater than  $10^{12} s^{-1}$ , making  $MV^{2+}$  an important new model system for exploring ultrafast ET in hydrogen-bonding donor solvents.

## Experimental Section

**Materials.** The dichloride salt of  $MV^{2+}$  was purchased from Aldrich and used as received. Some experiments were performed on counterion-exchanged salts prepared with either tetrafluoroborate ( $BF_4^-$ ) or hexafluorophosphate ( $PF_6^-$ ) counterions. The former salt is more soluble in water and short alcohols, whereas the latter salt is more soluble in acetonitrile. The hexafluorophosphate salt was prepared by addition of  $HPF_6$  to an aqueous solution of the chloride salt.<sup>33</sup> The white precipitate formed immediately upon mixing was filtered and washed several times with water. The tetrafluoroborate salt was prepared in similar fashion by adding  $AgBF_4$  to an aqueous solution of  $MV^{2+}(Cl^-)_2$ .

Solvents of the highest available purity were purchased from Aldrich or Burdick and Jackson and used as received. Water was obtained from a laboratory ultrapurifier (Barnstead Nanopure).  $D_2O$  (Aldrich) was 99.8% isotopically pure. For several experiments, acetonitrile was dried by refluxing over calcium hydride, which was followed by fractional distillation. The excellent agreement of transients obtained with and without this special drying procedure indicates that trace amounts of water have no significant effect on the dynamics.  $MV^{2+}$  salts are hygroscopic and readily form hydrates. Special measures to dry  $MV^{2+}$  were not taken in view of the fact that even ultrapure organic solvents contain trace quantities of water. No efforts were taken to deaerate the solutions under study since diffusion-limited quenching by the millimolar concentrations of oxygen present in organic solvents is much too slow to influence dynamics on the subnanosecond time scale of interest here.

**Femtosecond Transient Absorption.** Transient absorption measurements were performed using the apparatus described previously.<sup>34</sup> Briefly, a regeneratively amplified titanium sapphire laser system was used to generate 265 nm pump pulses,

approximately 150 fs in duration. Continuum generation in a 1 cm water cell provided tunable probe pulses from 390 to 1000 nm. Probe pulses at 270 nm were obtained from an ultraviolet continuum generated by focusing several hundred nJ of the laser second harmonic ( $\lambda = 398$  nm) in a 1 mm thick  $\text{CaF}_2$  plate. Pump and probe pulses were overlapped in a 500  $\mu\text{m}$  thick, free-standing jet of the solution under study. The pulses were linearly polarized and the angle between their planes of polarization was set to the magic angle ( $54.7^\circ$ ) to eliminate dynamics due to molecular reorientation. The instrumental response time was approximately 180 fs at most probe wavelengths, as determined by cross-correlation of pump and probe pulses in a BBO crystal.

Transient absorption signals were monitored at a fixed probe wavelength as a function of pump–probe delay time. After the sample, the probe pulse was directed through an  $f = 0.25$  m monochromator and detected by an amplified Si photodiode or a photomultiplier tube positioned at the exit slit. The slit width was adjusted to optimize the time resolution. The signal from the photodetector was sent to a lock-in amplifier (Stanford Research Systems) together with a reference signal from an optical chopper positioned in the pump beam. The output from the lock-in amplifier is directly proportional to the absorbance change induced in the probe pulse by the pump pulse. With this phase-sensitive detection technique our instrument is able to measure absorbance changes of less than  $10^{-4}$ .

Transient spectra were recorded by passing the entire continuum probe beam through the sample jet and into a monochromator. A lock-in amplifier detected the signal as the wavelength was scanned under computer control. During wavelength scanning the position of the optical delay line was adjusted to compensate for the group-delay dispersion of the probe pulse.<sup>35</sup>

All transient absorption signals in methanol and acetonitrile solutions were independent of laser power. It was verified that the signals changed linearly as the pump intensity was varied between 5 and 50  $\text{GW cm}^{-2}$ . In water, however, a weak offset due to two-photon ionization of the solvent was sometimes seen at long delay times after the solute signal had decayed away. This is described more fully in the results section.

**Time-Resolved Fluorescence.** Fluorescence decays were measured by time-correlated single-photon counting (TCSPC). By cavity dumping a synchronously pumped dye laser, picosecond pulses at 287 nm were generated at a repetition rate of 1 MHz and used to excite solutions held in a 1.0 cm cuvette. Fluorescence was collected at  $90^\circ$ , directed through a double monochromator (American Holographic), and detected by a microchannel-plate photomultiplier tube (Hamamatsu). The instrument response time was approximately 40 ps (fwhm).<sup>36</sup> All fluorescence transients were recorded at an emission wavelength of 350 nm. Lifetimes were determined by iterative deconvolution of a double-exponential model function with the instrument response.

**Steady-State Spectroscopy.** Steady-state fluorescence emission and excitation spectra were recorded with a commercial fluorimeter (Fluoromax-2, Spex Instruments). All spectra were corrected for the instrument's spectral response by calibration of the excitation monochromator using rhodamine 6G in ethanol as a quantum counter.<sup>37</sup> The optical density of all solutions was kept as low as possible to avoid the reabsorption of fluorescence. Emission measurements in acetonitrile were performed primarily with  $\text{MV}^{2+}(\text{PF}_6^-)_2$  which is considerably more soluble in this solvent than the dichloride salt. Measurements carried out on saturated solutions of  $\text{MV}^{2+}(\text{Cl}^-)_2$  gave identical results.

Absorption spectra were recorded with a conventional UV–vis spectrophotometer (Lambda 6, Perkin-Elmer). All measurements were carried out on room-temperature solutions ( $T = 22 \pm 1^\circ\text{C}$ ).

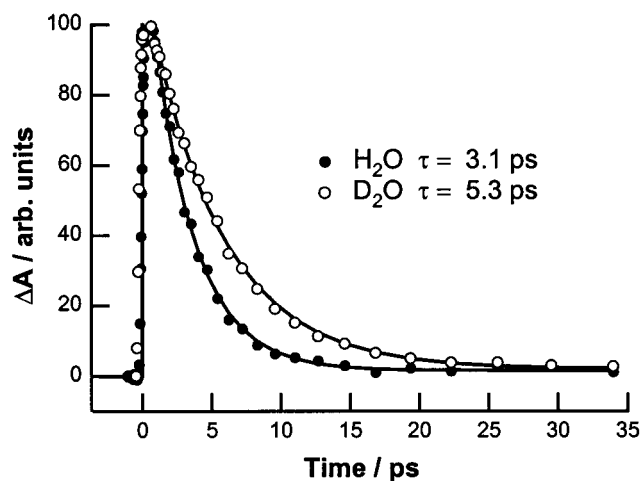
**Least-Squares Curve Fitting.** Transient absorption signals were fit to a sum of exponential functions using global analysis software written in our laboratory. Our software allows multiple transients to be fit simultaneously using a common model function. An arbitrary combination of the parameters of this function can be linked for any combination of the transients in the set. All remaining parameters are independently optimized for each transient. If  $n$  transients are simultaneously fit to a model function with  $m$  parameters, then the full parameter set is described by an  $n \times m$  matrix. In global fitting, an arbitrary set of these matrix elements can be linked (i.e., constrained to take on identical values), thus reducing the dimensionality of the full parameter space. For example, assume that the three parameter function  $a + be^{-kt}$  is used to simultaneously fit four transients. If the rate constant,  $k$ , is globally linked for all four, but the parameters  $a$  and  $b$  are allowed to take on unique values for each transient, then the total number of independent parameters is 9. Developed originally for analyzing time- and wavelength-resolved emission data,<sup>38,39</sup> global fitting is invaluable for analyzing two-dimensional data sets from transient absorption experiments. In particular, global fitting provides highly robust estimates of parameters such as exponential time constants that are common to a set of independently measured signals.<sup>40</sup> This situation occurs frequently in transient absorption experiments, where one or more transient species contribute to the probe absorption at multiple probe wavelengths. Our program uses the Marquardt–Levenberg algorithm for parameter estimation.<sup>41</sup> All derivatives are evaluated by finite differences.

The fitting function used in this study was a sum of exponentials analytically convoluted with a Gaussian function to represent the instrument response. The Gaussian fwhm was fixed at 180 fs based on cross-correlation measurements between the 265 nm pump pulse and the 600 nm probe pulse. Parameter uncertainties stated below are equal to twice the standard deviations determined by the fitting program.

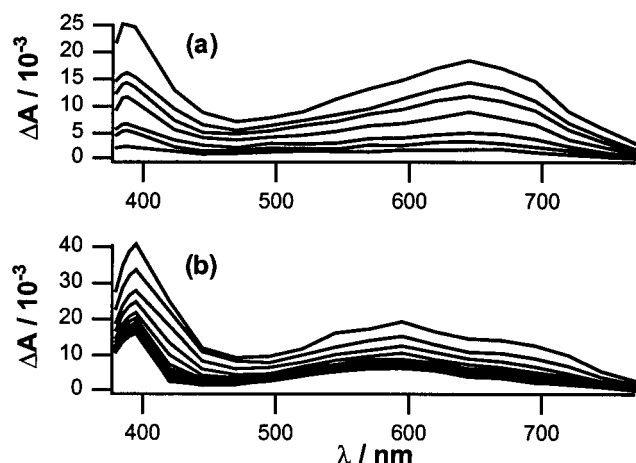
## Results

Figure 1 shows the absorbance change ( $\Delta A$ , equivalent to  $\Delta\text{OD}$ ) at 600 and 270 nm as a function of time after photoexcitation of a 2.3 mM solution of  $\text{MV}^{2+}(\text{Cl}^-)_2$  in methanol. The signal at 600 nm (open circles) shows an instrument-limited rise, followed by a rapid decay to an offset or plateau. The signal offset shows little decay up to 800 ps after the pump pulse, the longest delay studied. Similar dynamics were observed at probe wavelengths between 380 and 740 nm. After dividing each trace by its maximum amplitude, all agree within experimental error. Because the dynamics are independent of probe wavelength throughout this broad spectral window, scans at 7 separate probe wavelengths were globally fit to a single-exponential plus a constant term to model the offset. Fits were made to just the first 8 ps of data at each wavelength. The time constant was linked for all scans but the amplitude of the exponential term and the magnitude of the long-time offset were optimized independently. The description of the full data set by a common exponential time constant ( $\tau = 430 \pm 40$  fs) is excellent. Identical dynamics were observed in methanol for the  $\text{MV}^{2+}(\text{BF}_4^-)_2$  salt.

At a probe wavelength of 270 nm a bleach signal (negative absorbance change) is observed in methanol (triangles in Figure



**Figure 3.** Transient absorption at 600 nm for  $MV^{2+}(Cl^-)_2$  in  $H_2O$  (closed circles) and  $D_2O$  (open circles) after excitation by a 150 fs, 265 nm pump pulse. Lifetimes obtained from fits to a single-exponential function are indicated in the figure (solid curves).



**Figure 4.** (a) Evolution of the transient spectra for  $MV^{2+}(Cl^-)_2$  in  $H_2O$  at various delay times between 100 fs (uppermost curve) and 12 ps (lowest curve) after the pump pulse. (b) Transient spectra recorded in methanol from 200 fs (uppermost curve) to 3 ps (lowest curve) after the pump pulse. All spectra have been corrected for group-delay dispersion.

1). The 270 nm probe wavelength lies within the ground-state absorption band of  $MV^{2+}$  (see the steady-state absorption spectrum in Figure 6). The observed bleach is consistent with depopulation of the electronic ground state by the pump pulse. The maximum amount of bleaching appears within our time resolution and then recovers rapidly to a residual bleach that remains nearly constant for hundreds of picoseconds. The time constant that best fits the bleach recovery is the same as the time constant that characterizes the decay of the transient absorption at visible wavelengths. Thus, performing a global fit on the set of visible transients *plus* the bleach signal at 270 nm again gives a time constant of 430 fs. The fit is excellent at all wavelengths, indicating that the decaying signals in the visible reflect repopulation of the electronic ground state of  $MV^{2+}$ .

The open circles in Figure 2 show the transient spectrum recorded for  $MV^{2+}$  in methanol 2 ps after the pump pulse. This spectrum was corrected for group delay dispersion ("chirp") of the spectrally broad continuum pulse. The solid curve in Figure 2 shows the spectrum of one-electron reduced methyl viologen,  $MV^{•+}$ , in  $H_2O$ , which has been scaled for comparison with the transient spectrum. To record the spectrum shown by the solid

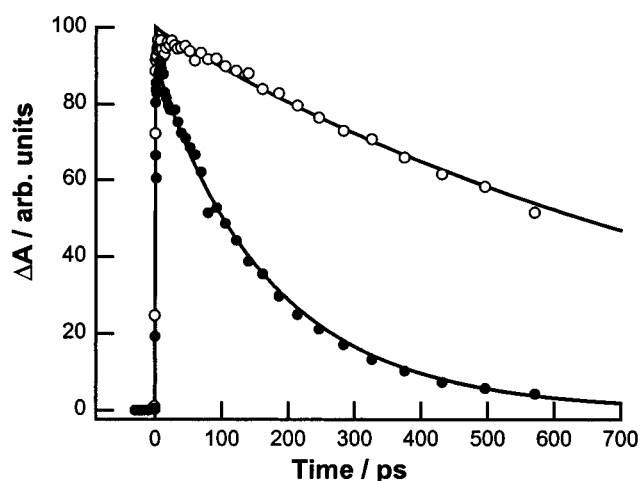


**Figure 5.** Transient absorption signal at 600 nm following 265 nm photoexcitation of  $MV^{2+}(PF_6^-)_2$  in acetonitrile (open circles) and in acetonitrile with 0.66 M of added  $H_2O$  (solid circles). Fits to time-resolved fluorescence decays at 350 nm (solid curves) are shown for the same two samples. The excellent agreement indicates that the 600 nm signal is due to excited-state absorption by the fluorescent singlet state of methyl viologen.

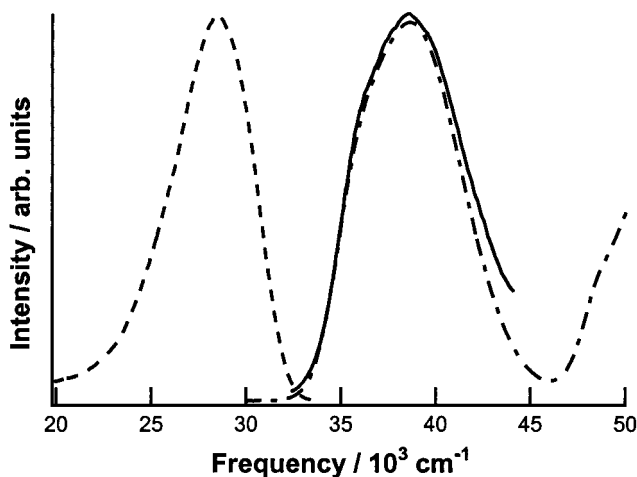


**Figure 6.** Steady-state emission spectrum of a  $5 \times 10^{-4}$  M solution of  $MV^{2+}(PF_6^-)_2$  in acetonitrile recorded at an excitation wavelength of 265 nm (dashed curve). The fluorescence excitation spectrum recorded at an emission wavelength of 350 nm (solid curve) is compared with the absorption spectrum of  $MV^{2+}(PF_6^-)_2$  in the same solvent (dot-dashed curve).

curve in Figure 2,  $MV^{•+}$  was generated by chemical reduction of an aqueous solution of  $MV^{2+}$  using Zn dust in a sealed, oxygen-free cuvette. The spectrum of this highly stable radical cation was then recorded with a conventional UV-vis spectrometer. The band maxima (396 and 606 nm) and characteristic vibrational structure are in complete agreement with literature findings.<sup>15</sup> The excellent agreement of this reference spectrum with the one from the pump-probe experiment in methanol leaves no doubt that the absorbing species in the plateau region of the signal is  $MV^{•+}$ .

Transient absorption at 600 nm is shown in Figure 3 for  $MV^{2+}$  in both  $H_2O$  and  $D_2O$ . The dynamics are considerably different than in methanol. In particular, the significant offset seen in methanol is absent, and the signal decays virtually to the baseline. Close inspection of the signals in Figure 3 reveals the presence of a weak ( $<1.5\%$  of the maximum amplitude) offset at long delay times. The offset varied quadratically as the pump pulse intensity was varied. In contrast, the decaying portion of the signal at short times varied linearly with pump intensity.



We therefore assign this weak signal contribution to absorption by hydrated electrons produced by two-photon ionization of the abundant water molecules. Water is a strong two-photon absorber in the UV<sup>42</sup> and can be efficiently two-photon ionized by femtosecond laser pulses.<sup>43</sup> A global fit to transients at several probe wavelengths in H<sub>2</sub>O gave a time constant of  $3.1 \pm 0.2$  ps. A best-fit time constant of  $5.3 \pm 0.4$  ps was obtained in D<sub>2</sub>O. Thus, the signals decay approximately 1 order of magnitude more slowly in water than in methanol.

Further differences between the dynamics in water and methanol are apparent when transient spectra recorded at various delay times are compared. Figure 4a shows transient spectra recorded 0–12 ps after the pump pulse in H<sub>2</sub>O, while Figure 4b shows transient spectra recorded between 0 and 3 ps in methanol. All spectra have been corrected for group-delay dispersion of the probe pulse. In both solvents, two absorption bands are observed that decay with the same time constant at all wavelengths. The spectrum in methanol matches the well-known spectrum of MV<sup>•+</sup> (compare with Figure 2) as mentioned above. The spectrum in water, although qualitatively similar to the spectrum of MV<sup>•+</sup>, shows some significant differences. In water, the band maxima occur at 388 and 644 nm. Relative to the spectrum of MV<sup>•+</sup>, the short wavelength absorption band is slightly blue-shifted, and the long wavelength absorption band is red-shifted. The ratio of the spectral amplitudes at the two band maxima is closer to 2:1 in water than the 3:1 ratio observed in methanol. There is no evidence of spectral shifting with time in either solvent, nor do any new bands appear during the decay of the initial two bands. Instead, the transient spectra agree at all delay times, justifying a global fit to the transients using a single-exponential time constant for each solvent. Finally, it should be noted that the transient species in water decays to the baseline, whereas the MV<sup>•+</sup> signal in methanol persists for hundreds of picoseconds following the conclusion of the 430 fs decay. Actually, a small decrease in the amplitude of the offset in methanol was detected between 2 and 50 ps after the pump pulse. Fitting the methanol scans over the entire 800 ps of delay required a second exponential with a time constant of approximately 10 ps. The amplitude of this decay is small, and could reflect geometrical rearrangement or vibrational cooling in the newly formed radical cation.

Upon changing the solvent to acetonitrile, the excited-state dynamics of MV<sup>2+</sup> change dramatically again. As shown in Figure 5 (open circles), the transient absorption at 600 nm decays very slowly in hundreds of picoseconds. This slow decay is in stark contrast to the several picosecond decay seen in water and the even faster dynamics in methanol. The data in Figure 5 were recorded for a solution of the hexafluorophosphate salt (MV<sup>2+</sup>(PF<sub>6</sub><sup>-</sup>)<sub>2</sub>) of methyl viologen because it is significantly more soluble in acetonitrile than the chloride salt. Transients were also recorded for a saturated solution of the chloride salt in acetonitrile, and no significant differences were observed. A transient spectrum recorded 100 ps after the pump pulse in acetonitrile is shown by the dashed curve in Figure 2. The shape of this spectrum is independent of delay time and agrees within experimental error with the transient spectrum recorded in water, which is shown in Figure 4a.

During the pump–probe experiments in acetonitrile, pale-blue fluorescence was visible by eye in the pumped volume of the jet. This observation coupled with the slow (~1 ns) decay of the transient absorption suggested to us the existence of a radiative decay pathway for electronically excited MV<sup>2+</sup> in acetonitrile. Fluorescence was confirmed by time-resolved and steady-state emission measurements. A fluorescence lifetime of

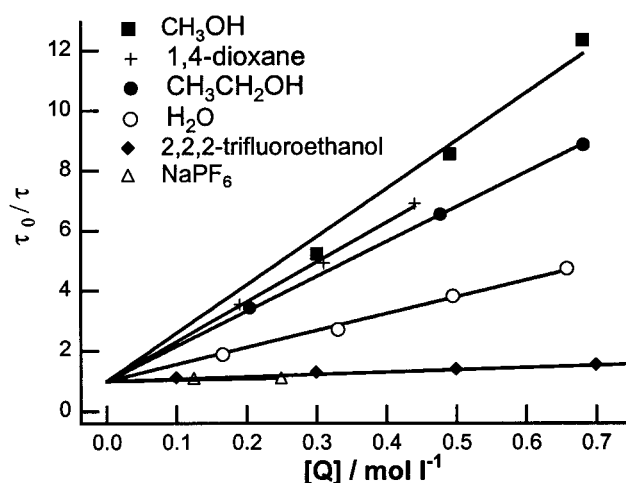


**Figure 7.** Stern–Volmer plot showing quenching of MV<sup>2+</sup>(PF<sub>6</sub><sup>-</sup>)<sub>2</sub> fluorescence in acetonitrile as determined by time-correlated single-photon counting experiments. The ratio of the fluorescence lifetime in the neat solvent,  $\tau_0 = 1.00$  ns, over the lifetime at finite quencher concentration,  $\tau$ , is plotted vs quencher concentration,  $[Q]$ . Solid curves are the result of linear-least-squares fitting to the expression,  $\tau_0/\tau = 1 + K_{SV}[Q]$ , where  $K_{SV}$  is the Stern–Volmer quenching constant. See Table 1 for a summary of the quenching rates calculated from the  $K_{SV}$  values.

$1.00 \pm 0.04$  ns was determined for methyl viologen in acetonitrile using the TCSPC technique. The solid line in Figure 5 shows the deconvoluted fit to the TCSPC emission decay, scaled for comparison with the transient absorption signal (open circles in Figure 5). The excellent agreement demonstrates that the pump–probe signal arises from excited state absorption by the fluorescent excited state. Because the existence of emission from electronically excited MV<sup>2+</sup> in fluid solution has been controversial in the past (see the discussion section), we also performed steady-state measurements with a conventional fluorimeter. Figure 6 summarizes the results obtained for a  $5 \times 10^{-4}$  M solution of MV<sup>2+</sup>(PF<sub>6</sub><sup>-</sup>)<sub>2</sub> in acetonitrile. The emission spectrum ( $\lambda_{exc} = 266$  nm) is shown by the dashed curve. The excitation spectrum of fluorescence detected at 350 nm is shown by the solid curve. Agreement with the ground-state absorption spectrum shown by the dot–dashed curve in Figure 6 is excellent, demonstrating that the solute is responsible for the emission.

Prolonged exposure to UV light resulted in very weak emission at wavelengths greater than 400 nm. We believe this emission arises from small amounts of pyridones formed in the presence of oxygen as reported previously.<sup>44,45</sup> By minimizing the UV flux, luminescence from these oxidation products was negligible, and oxygen-free conditions were unnecessary. The fluorescence quantum yield was determined to be  $0.03 \pm 0.01$  by comparison with 9,10-diphenylanthracene in cyclohexane ( $\phi_f = 0.85$ , independent of excitation wavelength<sup>46</sup>). Identical results were obtained from a saturated solution of the considerably less soluble chloride salt of MV<sup>2+</sup>. No fluorescence could be detected in acetonitrile solutions of the monopyridinium compounds pyridinium chloride and *N*-methylpyridinium chloride.

The observation of MV<sup>2+</sup> fluorescence in acetonitrile allowed us to study diffusional fluorescence quenching. Fluorescence lifetimes were measured for various concentrations of added quenchers using the TCSPC apparatus. Quenchers were selected that do not absorb significantly at the pump wavelength of 287 nm in order to simplify the analysis. Figure 7 shows a Stern–Volmer plot summarizing the quenching results. Quenching rates and gas-phase ionization potentials for the various quenchers

**TABLE 1: Bimolecular Quenching Rates ( $k_q$ ) of Methyl Viologen Fluorescence in Acetonitrile<sup>a</sup>**

quencher	$k_q/10^{10} \text{ M}^{-1} \text{ s}^{-1}$	IP/eV
methanol	1.6	10.84
1,4-dioxane	1.3	9.19
ethanol	1.3	10.48
H <sub>2</sub> O	0.70	12.62
2,2,2-trifluoroethanol	0.075	11.5
NH <sub>4</sub> PF <sub>6</sub>	0.040	<i>b</i>
CCl <sub>4</sub>	<i>c</i>	11.47
CHCl <sub>3</sub>	<i>c</i>	11.37

<sup>a</sup>  $k_q$  values were obtained from Stern–Volmer analysis using  $\tau_0 = 1.00$  ns in neat acetonitrile. IP is the gas-phase ionization potential in eV from ref 53. <sup>b</sup> No value reported. <sup>c</sup> The fluorescence lifetime increased slightly as the quencher concentration was increased from 0 to 1 M.

are summarized in Table 1. For several quenchers Stern–Volmer constants were determined both from TCSPC measurements of fluorescence decay times and from the integrated, steady-state emission intensity measured with a fluorimeter. The constants obtained by these two different methods agree within experimental error, indicating the absence of significant static quenching.

Our primary aim was to determine what kinds of compounds give rise to significant fluorescence quenching. For this reason, we have ignored subtleties of the quenching curves such as the presence of upward or downward curvature, and have simply fit all points to a straight line. From this analysis, the quenchers shown in Figure 7 can be divided into three categories. The first category includes molecules like the alcohols and 1,4-dioxane that quench at approximately diffusion-limited rates. In the second category are compounds that show minimal quenching. These include the salt NaPF<sub>6</sub>, trifluoroethanol, chloroform, and carbon tetrachloride. The quenching rate of water falls somewhere between these two limits and constitutes a category by itself.

## Discussion

**Fluorescence in Acetonitrile.** The discovery of a significant quantum yield for emission in acetonitrile was not anticipated because it has been frequently stated that methyl viologen does not fluoresce in fluid solution.<sup>12,26,32,45,47</sup> Several investigators suggested otherwise<sup>48,49</sup> but these reports have been controversial.<sup>50</sup> Although MV<sup>2+</sup> has been used in acetonitrile in the past for other purposes,<sup>2,51</sup> the luminescence described here appears not to have been reported previously.

Although this is the first report of a significant radiative decay pathway for MV<sup>2+</sup> in fluid solution, there have been a few reports of fluorescence in other media. Fluorescence was reported by Villemure et al. for MV<sup>2+</sup> incorporated into the interlamellar spaces of hectorite and montmorillonite clays suspended in water.<sup>49</sup> In the same communication, Villemure et al. described much weaker emission from MV<sup>2+</sup> in aqueous solution. The author's emission spectrum ( $\lambda_{\text{max}} = 345$  nm) agrees very well with the spectrum we observed in acetonitrile (Figure 6). We also performed emission measurements on MV<sup>2+</sup> in water and had no difficulty observing a weak emission spectrum with the same spectral shape as the more intense emission seen in acetonitrile. The fluorescence Stokes shift is thus very similar in both solvents, suggesting that the ground and excited singlet states are stabilized in a similar manner. Finally, we note that significantly more intense emission has been observed for related bipyridinium compounds in water. Hopkins et al. reported a quantum yield of  $0.04 \pm 0.02$  and a

fluorescence lifetime of 1.6 ns for 1,1'-ethylene-2,2'-bipyridinium dibromide (common name, diquat) in aqueous solution.<sup>23</sup> Mau et al. reported a fluorescence quantum yield of 0.081 and a fluorescence lifetime of  $0.48 \pm 0.01$  ns for 1,1',2,2',6,6'-hexamethyl-4,4'-bipyridinium, also known as hexamethyl viologen.<sup>45</sup> The fluorescent nature of the latter compounds shows that there is no inherent reason fluorescence cannot be observed from viologens.

Fluorescence from electronically excited methyl viologen (MV<sup>2+\*</sup>) was reported in zeolite hosts such as NaY and other alkaline ion faujasites by Alvaro et al.<sup>11,12</sup> Two emission bands were seen; a weak band with  $\lambda_{\text{max}} = 340$  nm and a more intense band with  $\lambda_{\text{max}} = 420$  nm. Both the emission maximum of the short wavelength band and the reported fluorescence lifetime of 1–2 ns<sup>12</sup> agree well with our results in acetonitrile. In their first report, Alvaro et al. suggested that the long-wavelength emission arises from a nonplanar conformer twisted around the inter-ring bond.<sup>11</sup> Later, the same authors reported that the excitation spectrum of the long-wavelength emission is strongly red-shifted from the ground-state absorption spectrum of MV<sup>2+</sup>.<sup>12</sup> Alvaro et al. suggested that the long-wavelength emission arises from complexation with the basic lattice since the 420 nm emission was more intense in the more basic zeolites.<sup>12</sup> In 1984, Thomas et al. reported long-wavelength emission from MV<sup>2+</sup>-anion complexes in fluid solution.<sup>48</sup> They assigned this emission to MV<sup>2+</sup>, but a later study by Mau et al. provided convincing evidence that this emission is due to minor amounts of oxidation products, especially pyridones.<sup>45</sup> Highly fluorescent pyridones can be formed by photolysis<sup>45</sup> of viologens and by thermal reaction with aqueous base in the presence of oxygen.<sup>44</sup> We believe that the long wavelength emission seen in the zeolites originates from similar oxidation products. Regardless of the origin of the long-wavelength emission, we can confidently assign the short-wavelength emission seen in zeolites to the same fluorescent transition seen in acetonitrile.

The weak emission seen in water, the much stronger emission seen in clays and zeolites, and the emission reported here for the first time in acetonitrile definitively establish a radiative decay pathway for the singlet excited state of methyl viologen. The common property of these diverse hosts is resistance to one-electron oxidation. This prevents ET quenching of electronically excited MV<sup>2+</sup>, allowing fluorescence to become the rate-limiting step for excited-state decay. The strong electron accepting character of MV<sup>2+\*</sup> can be placed on a more quantitative basis. The high singlet energy and favorable reduction potential of ground-state MV<sup>2+</sup> make MV<sup>2+\*</sup> a formidable oxidant. Following standard practice, we estimate the singlet energy to be 4.10 eV from the intersection of the corrected emission and absorption spectra at 302 nm. Combining this value with the ground-state reduction potential of  $-0.45$  V vs NHE<sup>20</sup> the excited-state reduction potential,  $E^\circ$  (MV<sup>2+\*/</sup>MV<sup>•+</sup>), is determined to be 3.65 V. This is an unusually high value for a closed-shell organic compound, and is the reason electron-transfer quenching of MV<sup>2+\*</sup> is a major deactivation pathway. In strongly polar solvents, the Coulomb energy between ET products can be neglected and electron transfer to MV<sup>2+\*</sup> should be exothermic for donors with oxidation potentials less positive than about 3.7 V. Relatively few oxidation potentials are accurately known above 3 V, so we estimated the feasibility of electron-transfer quenching using an empirical relation due to Miller<sup>52</sup>

$$E^\circ = 0.89 \text{ IP} - 5.50 \text{ (vs NHE)} \quad (1)$$

In this relation,  $E^\circ$  is the one-electron oxidation potential in Volts and IP is the gas-phase ionization potential in eV. Although this correlation is approximate, it provides a zeroth-order prediction that species with gas-phase ionization potentials  $\leq 10.3$  eV will be one-electron oxidized by electronically excited methyl viologen. This is in good accord with the fluorescence quenching results in Table 1. As shown in Table 1, compounds with gas-phase IPs less than 10.8 eV quench  $MV^{2+}$  efficiently, whereas those with higher IPs do not.

Acetonitrile has an IP of 12.20 eV<sup>53</sup> and is unable to quench  $MV^{2+}$  by electron transfer. The high resistance of acetonitrile to oxidation is of course the reason for its extensive use as a solvent in electrochemistry. Using the Miller relation (eq 1), the oxidation potential of acetonitrile is predicted to be 5.4 V vs NHE, in good agreement with an experimental value of 5.0 V vs NHE measured using a microelectrode.<sup>54</sup> The  $E^\circ$  value of acetonitrile thus lies significantly above  $E^\circ(MV^{2+}/MV^{\bullet+}) = 3.65$  V and ET quenching by oxidation of acetonitrile is thermodynamically uphill. As a result, fluorescence becomes an observable decay pathway.

Because the transient signals from  $MV^{2+}$  in acetonitrile decay at precisely the same rate as the fluorescence, the transient absorption must be due to transitions from the fluorescent state,  $S_1$ , to higher-lying singlet states,  $S_N$ . Thus, the transient spectrum recorded in acetonitrile 100 ps after the pump pulse (dashed curve in Figure 2) is assigned to  $S_1 \rightarrow S_N$  absorption by  $MV^{2+}$ . This spectrum is qualitatively similar to the spectrum of  $MV^{\bullet+}$ , as expected from elementary molecular orbital theory. Because the highest occupied orbital of the excited singlet state of  $MV^{2+}$  is the same as the singly occupied orbital of the radical cation, the two species have a number of energetically comparable transitions. Similar trends are seen for 4,4'-bipyridine. The  $S_1 \rightarrow S_N$  spectrum of this neutral molecule strongly resembles the spectrum of its radical anion. The  $S_1 \rightarrow S_N$  spectrum of 4,4'-bipyridine has  $\lambda_{\max} = 378, 590$  nm,<sup>55</sup> whereas the radical anion has maximum absorption at  $\lambda_{\max} = 381$  nm, 570 nm.<sup>56</sup> The changes in absorption peak heights and the shifts in peak positions upon reduction of 4,4'-bipyridine agree well with the changes in the spectra of  $MV^{2+}$  vs  $MV^{\bullet+}$ . This close correspondence is expected since 4,4'-bipyridine is  $\pi$ -isoelectronic with  $MV^{2+}$ .

**Dynamics in Water.** Like acetonitrile, water has a high gas-phase ionization potential (12.62 eV<sup>53</sup>) and ET quenching of  $MV^{2+}$  is not observed.<sup>57</sup> In water, however, the fluorescence lifetime inferred from the decay of the excited state absorption signals is over 300 $\times$  shorter than in acetonitrile. The emission and transient absorption spectra observed in water match the ones seen in acetonitrile very closely. In particular, there is no evidence for photoreduction at any time. As in the case of acetonitrile, the signal is assigned to absorption by the  $S_1$  state.

Several observations indicate that nonradiative decay of  $MV^{2+}$  can occur by a mechanism other than electron transfer.<sup>58</sup> First of all, the fluorescence quantum yield in acetonitrile is small ( $\phi_F = 0.03$ ), indicating that most excited states decay nonradiatively. There is no evidence for reductive quenching in this system, so there must be an additional nonradiative decay channel. As pointed out in the results section, fluorescence could not be observed from the monopyridinium compound *N*-methylpyridinium in acetonitrile. According to Mariano, this compound's excited-state reduction potential is +3.0 V,<sup>59</sup> and reductive quenching by acetonitrile can again be ruled out. It thus appears that nonradiative decay by a non-ET process may be a common deactivation pathway for mono- and bipyridinium compounds. In water, this nonradiative decay channel has a

much higher rate than in acetonitrile. As both solvents are already highly polar, it seems unlikely that such a pronounced lifetime difference could arise from a solvent polarity-dependent barrier. The observed kinetic isotope effect of 1.7 implicates a proton coordinate in the excited-state deactivation, and yet there are no plausible protonation or deprotonation sites for  $MV^{2+}$ .<sup>60</sup> Furthermore, the good proton-donor alcohol, 2,2,2-trifluoroethanol (TFE), does not significantly quench  $MV^{2+}$  fluorescence in acetonitrile (see Table 1). The gas-phase ionization potential of TFE is greater than 11.5 eV,<sup>53</sup> precluding the possibility of ET.

The Stern–Volmer result provides another clue to the nature of the rapid nonradiative decay observed in water. Because there is no evidence for water clustering in acetonitrile–water binary solvents when the acetonitrile fraction is higher than 0.8,<sup>61</sup> our quenching results strongly suggest that a single water molecule is able to deactivate the excited state. One possible deactivation pathway involves isomerization. Chachisvilis and Zewail have suggested that ultrafast isomerization via a conical intersection causes the ultrafast deactivation of electronically excited pyridinium ion.<sup>62</sup> Perhaps a single water molecule can control access to the conical intersection that is responsible for isomerization. Alternatively, the water molecule could itself be a reactant in an as yet uncharacterized photoreaction of  $MV^{2+}$ . In preliminary experiments, we have detected a residual transient absorption near 300 nm in bulk water that may be assignable to an  $MV^{2+}$  isomer or a novel photoproduct. These results will be presented in more detail elsewhere.<sup>63</sup>

**Ultrafast Photoreduction in Methanol.** ET quenching of  $MV^{2+}$  dominates the pump–probe signals in methanol. Direct evidence for this comes from the unequivocal detection of  $MV^{\bullet+}$  following 265 nm excitation. Transient spectra recorded every 200 fs from 0 to 4 ps (Figure 4b) show no discernible reshaping and match the spectrum of  $MV^{\bullet+}$  at all delay times. This indicates that forward electron transfer generates  $MV^{\bullet+}$  faster than our instrumental time response of  $\sim 180$  fs. Our data thus show that photoreduction in methanol occurs on an ultrafast time scale.

The bleach recovery seen at 270 nm provides the key to interpreting the 430 fs time constant observed at all probe wavelengths. Spectra published by Watanabe et al.<sup>15</sup> indicate that  $MV^{2+}$  has a greater extinction coefficient at 270 nm than  $MV^{\bullet+}$ . This fact explains the initial bleach, assuming that these are the only two species that contribute to the signal. As already noted in the results section, the bleach signal at 270 nm is fit by the same 430 fs time constant that characterizes the signal decays at longer wavelengths. We therefore assign the rapid decay of the signals in the visible to decay of the  $MV^{\bullet+}$  population by back ET. Back ET causes a concomitant increase of the  $MV^{2+}$  ground-state population, resulting in the bleach recovery seen at 270 nm. Thus, forward ET at a rate faster than our time resolution, followed by back ET on the subpicosecond time scale, provides a consistent explanation of the pump–probe data in methanol. Back ET occurs at a rate in excess of  $10^{12}$  s<sup>-1</sup> despite the fact that this reaction is likely to be strongly Marcus-inverted. In the past, the ultrafast solvation response of liquids has been cited as a key to understanding the high rates of nominally Marcus-inverted ET reactions.<sup>64</sup> More detailed discussion of the ET dynamics will be presented elsewhere.<sup>65</sup>

Particularly noteworthy is the observation that back ET is not 100% efficient in the  $MV^{2+}$ /methanol system despite the very high rates of charge transfer and charge recombination. Because  $MV^{\bullet+}$  is the only species contributing to the pump–



probe signals at visible probe wavelengths, the photoreduction yield can be calculated by the ratio of the signal in the plateau region to its initial value near  $t = 0$ . The yield in methanol determined by this method is  $12 \pm 3\%$ . This value was calculated using parameters from the least-squares fits (i.e., deconvoluted values) in order to obtain an estimate that is unbiased by the finite instrument response of our spectrometer.

**Identity of the Electron Donor in Methanol.** The ionization potential of methanol is 10.84 eV.<sup>53</sup> This value is higher than the maximum IP for ET quenching of  $MV^{2+*}$  of 10.3 eV predicted by the Miller correlation (eq 1). We therefore considered the possibility that the electron donor is not a solvent molecule but is instead a chloride counterion. Ebbesen and co-workers studied  $MV^{2+}(Cl^-)_2$  solutions that were 1 or 2 M in added NaCl.<sup>30–32</sup> Under these conditions, ion association is strongly favored and these authors observed electron donation from a chloride counterion. Halide ions quench the fluorescence of many aromatic species, including fluorescence from the bipyridinium compound diquat.<sup>23</sup> The appearance of  $MV^{•+}$  less than 180 fs after the pump pulse in our experiments indicates however that the electron donor must be in close proximity to the excited  $MV^{2+}$  ion because diffusional encounter of free ions is impossible on this time scale. Thus, electron transfer from a chloride counterion is conditional on extensive  $MV^{2+}$ -counterion association. In dilute solution, ion association can give rise to contact or solvent-separated ion pairs, either of which could serve as the electron donor in the ultrafast photoreduction of  $MV^{2+}$ .

The key question is then whether  $MV^{2+}$ -counterion association occurs for the millimolar salt concentrations used in our experiments. Equilibrium constants for  $MV^{2+}$ -counterion association in water are of the order of  $1\text{ M}^{-1}$ ,<sup>66</sup> implying that  $MV^{2+}$  should be present predominantly as free ions in this solvent. Ion association generally increases as the solvent dielectric constant decreases,<sup>67</sup> so more association should occur in solvents less polar than water. However, we found that neither the fluorescence lifetime nor the quantum yield of emission changed in acetonitrile when the concentration of  $MV^{2+}$  was varied between  $10^{-4}\text{ M}$  and  $10^{-3}\text{ M}$ . From this result, we conclude that  $MV^{2+}$  is a strong electrolyte at millimolar concentrations in acetonitrile.

Because acetonitrile and methanol have similar dielectric constants the absence of ion pairing in the former suggests that  $MV^{2+}$  exists only as free ions in the latter solvent. To be certain that the chloride ions do not play a role in the photoreduction dynamics reported here, experiments were performed with tetrafluoroborate and hexafluorophosphate salts of methyl viologen. Several considerations strongly indicate that these counterions cannot be oxidized by the excited state of  $MV^{2+}$ . First of all, the resistance of these ions to oxidation is responsible for their use for many years to extend the anodic potential range of electrochemical measurements in acetonitrile.<sup>68</sup> Second, these anions are predicted to have unusually high photodetachment energies in the gas phase<sup>69,70</sup> and even higher photodetachment thresholds in a polar solvent. Finally, addition of  $NaPF_6$  did not significantly quench  $MV^{2+}$  fluorescence in acetonitrile (see Table 1). The small decrease in the fluorescence lifetime that was observed can be attributed to the changing ionic strength of the solution.

The  $BF_4^-$  and  $PF_6^-$  anions are strongly stabilized by delocalization of the excess charge over multiple electron-affinic fluorine atoms. For this reason, the corresponding neutral species have been aptly termed “superhalogens”<sup>70,71</sup> because they have higher electron affinities than chlorine, the element with the

highest electron affinity. Ab initio calculations predict a vertical detachment energy of 7.35 eV for  $PF_6^-$ <sup>69</sup> and an adiabatic electron affinity of 6.75 eV for  $BF_4^-$ .<sup>70</sup> The gas-phase electron affinities of both species are therefore predicted to be more than 3 eV greater than atomic chlorine. Although experimental values are not available for  $BF_4^-$  and  $PF_6^-$ , recent experimental work has confirmed the ability of the ab initio methods to predict ion energetics for a closely related family of superhalogens.<sup>72</sup> Upon moving a negative ion with a positive electron affinity from the gas-phase to a polar solvent like acetonitrile, the photodetachment threshold of the negative ion is increased significantly due to polar solvation.<sup>73,74</sup> Use of the Born equation<sup>75</sup> together with estimates of the ionic radii predicts that the detachment thresholds should increase by several eV in polar solvents like acetonitrile and methanol. In contrast, the ionization threshold of a comparably sized neutral species decreases by the same amount in a polar solvent due to the stabilization of the upper cation state. All evidence indicates that the  $BF_4^-$  and  $PF_6^-$  ions cannot be oxidized by  $MV^{2+*}$ . Experiments on salts containing these ions therefore eliminate the possibility of reductive quenching by an associated counterion.

Identical dynamics were observed in methanol for both the chloride and the tetrafluoroborate salts of  $MV^{2+}$ . Thus, the counterion plays no role in the photoreduction dynamics, and the electron donor must be a solvent molecule.<sup>76</sup> Addition of methanol to  $MV^{2+}$  in acetonitrile led to diffusional fluorescence quenching (see Table 1). This further indicates that methanol is one-electron oxidized by the  $S_1$  state of  $MV^{2+}$ . The results presented here show that  $MV^{2+}$  in methanol is a novel example of ultrafast intermolecular ET in an electron-donating solvent. Yoshihara and co-workers have studied this type of ET reaction in great detail.<sup>77–79</sup> In these pioneering experiments, a solvent molecule in the vicinity of an electronically excited acceptor is the electron donor. Because it is not necessary for the two ET partners to diffuse together prior to reaction, it has been possible to study intrinsic bimolecular ET rates in these systems. In addition, the dual role of the solvent as both redox partner and solvating medium has led to many interesting tests of ultrafast ET theories.

Because of the weakly oxidizing character of the photoexcited acceptors used previously, relatively strong electron-donating solvents have been employed. Thus, most of the experiments carried out to date have used substituted aniline solvents. The work presented here shows that the very high oxidizing power of  $MV^{2+*}$  allows electron donation to be observed in methanol. Photooxidation of weak electron donors like alcohols normally requires powerful metal ion or radical oxidants. Unlike the relatively nonpolar electron-donor solvents used in the past, methanol is highly polar and therefore allows the effects of solvent polarity on ultrafast ET to be studied for the first time. More importantly, the hydrogen-bonded character of methanol can be expected to have a strong effect on the ET dynamics. In particular, the hydrogen-bonded donor solvent leads to coupling between electron and proton transfer. We will report elsewhere on our use of  $MV^{2+}$  in alcohols to study these couplings.<sup>65</sup>

## Conclusions

We have presented the first pump–probe investigation with femtosecond time resolution of the excited state dynamics of a bipyridinium compound. Unexpectedly diverse behavior was found for the excited state dynamics of methyl viologen in different polar solvents. In acetonitrile, fluorescence was observed for the first time. In water, the fluorescence lifetime



is shortened by a factor of approximately 300 due to a nonradiative decay channel that does not involve ET. This channel shows a kinetic isotope effect of 1.7. A variety of donors efficiently quench  $MV^{2+}$  fluorescence in acetonitrile. This study demonstrates that  $MV^{2+}$  is a potent photooxidant. The high singlet energy and favorable ground-state reduction potential combine to yield an excited-state reduction potential of  $E^\circ(MV^{2+*}/MV^{*+}) = +3.65$  V, an unusually high value for a closed-shell, aromatic compound. ET quenching of the singlet excited state has been shown to be the dominant deactivation channel in many environments. Electron transfer from the solvent in methanol reductively quenches the singlet excited state of this closed-shell, organic dication. Pump–probe measurements on superhalide salts of  $MV^{2+}$  definitively establish methanol as the electron donor. The rate of forward electron transfer is faster than our time resolution ( $\sim 180$  fs). Decay of  $MV^{*+}$  occurs with a characteristic time constant of 430 fs. Both forward and back ET rates are considerably faster than the inverse solvation time of methanol, and both steps constitute ultrafast ET reactions. Despite ultrafast back ET, a finite yield (“free ion yield”) of about 12% is observed for the ET products 2 ps after the pump pulse. Because the electron donor is a hydrogen-bonded solvent, we anticipate that this novel ultrafast ET system will provide insight into couplings between electron and proton-transfer reactions in polar solvents.

**Acknowledgment.** Helpful discussions with Professors Bruce S. Hudson, Michael A. J. Rodgers, and J. Kerry Thomas are gratefully acknowledged. We thank Professor Claudia J. Turro for advice on the preparation of the counterion-exchanged salts of methyl viologen and Kristin M. Huchton for her measurement of fluorescence quenching by trifluoroethanol. Finally, we thank Prof. Terry L. Gustafson for generously making his TCSPC apparatus available to us.

## References and Notes

- (1) A number of applications of methyl viologen are described in a general review article by Summers on bipyridines and their derivatives [Summers, L. A. *Adv. Heterocyc. Chem.* **1984**, 35, 281].
- (2) Sullivan, B. P.; Dressick, W. J.; Meyer, T. J. *J. Phys. Chem.* **1982**, 86, 1473.
- (3) Borja, M.; Dutta, P. K. *Nature* **1993**, 362, 43.
- (4) Alam, M. M.; Ito, O. *J. Phys. Chem. A* **1999**, 103, 1306.
- (5) Konigstein, C. J. *Photochem. Photobiol. A* **1995**, 90, 141.
- (6) Fromherz, P.; Rieger, B. *J. Am. Chem. Soc.* **1986**, 108, 5361.
- (7) Mao, Y.; Breen, N. E.; Thomas, J. K. *J. Phys. Chem.* **1995**, 99, 9909.
- (8) Brun, A. M.; Harriman, A. *J. Am. Chem. Soc.* **1991**, 113, 8153.
- (9) Colmenarejo, G.; Gutierrez-Alonso, M. C.; Barcena, M.; Kelly, J. M.; Montero, F.; Orellana, G. *J. Biomolecular Struct. Dyn.* **1995**, 12, 827.
- (10) Dunn, D. A.; Lin, V. H.; Kochevar, I. E. *Biochem.* **1992**, 31, 11 620.
- (11) Alvaro, M.; Facey, G. A.; Garcia, H.; Garcia, S.; Scaiano, J. C. *J. Phys. Chem.* **1996**, 100, 18173.
- (12) Alvaro, M.; Garcia, H.; Garcia, S.; Marquez, F.; Scaiano, J. C. *J. Phys. Chem. B* **1997**, 101, 3043.
- (13) Das, S. K.; Dutta, P. K. *Langmuir* **1998**, 14, 5121.
- (14) Marcello, V.; Castagnola, N. B.; Ortins, N. J.; Brooke, J. A.; Vaidyahlingam, A.; Dutta, P. K. *J. Phys. Chem. B* **1999**, 103, 2408.
- (15) Watanabe, T.; Honda, K. *J. Phys. Chem.* **1982**, 86, 2617.
- (16) Chitose, N.; LaVerne, J. A.; Katsumura, Y. *J. Phys. Chem. A* **1998**, 102, 2087.
- (17) Solar, S.; Solar, W.; Getoff, N. *J. Chem. Soc., Faraday Trans. 1* **1984**, 80, 2929.
- (18) Yonemoto, E. H.; Saupe, G. B.; Schmehl, R. H.; Hubig, S. M.; Rile, R. L.; Iverson, B. L.; Mallouk, T. E. *J. Am. Chem. Soc.* **1994**, 116, 4786.
- (19) Nishimura, Y.; Misawa, H.; Sakuragi, H.; Tokumaru, K. *Chem. Lett.* **1989**, 1555.
- (20) Wardman, P. *J. Phys. Chem. Ref. Data* **1989**, 18, 1637.
- (21) Julliard, M.; Chanon, M. *Chem. Rev.* **1983**, 83, 425.
- (22) Kavarnos, G. J.; Turro, N. J. *Chem. Rev.* **1986**, 86, 401.
- (23) Hopkins, A. S.; Ledwith, A.; Stam, M. F. *Chem. Commun.* **1970**, 494.
- (24) Ledwith, A. *Acc. Chem. Res.* **1972**, 5, 133.
- (25) McManus, H. J. D.; Finel, C.; Kevan, L. *Radiat. Phys. Chem.* **1995**, 45, 761.
- (26) Barnett, J. R.; Hopkins, A. S.; Ledwith, A. *J. Chem. Soc., Perkin Trans. 2* **1973**, 80.
- (27) Blacker, A. J.; Jazwinski, J.; Lehn, J.-M. *Helv. Chim. Acta* **1987**, 70, 1.
- (28) Knapp, C.; Lecomte, J.-P.; Kirsch-De Mesmaeker, A.; Orellana, G. *J. Photochem. Photobiol. B: Biol.* **1996**, 36, 67.
- (29) Rodgers, M. A. J. *Photochem. Photobiol.* **1979**, 29, 1031.
- (30) Ebbesen, T. W.; Levey, G.; Patterson, L. K. *Nature* **1982**, 298, 545.
- (31) Ebbesen, T. W.; Ferraudi, G. *J. Phys. Chem.* **1983**, 87, 3717.
- (32) Ebbesen, T. W.; Manring, L. E.; Peters, K. S. *J. Am. Chem. Soc.* **1984**, 106, 7400.
- (33) Bockman, T. M.; Kochi, J. K. *J. Org. Chem.* **1990**, 55, 4127.
- (34) Peon, J.; Hess, G. C.; Pecourt, J.-M. L.; Yuzawa, T.; Kohler, B. *J. Phys. Chem. A* **1999**, 103, 2460.
- (35) Klimov, V. I.; McBranch, D. W. *Opt. Lett.* **1998**, 23, 277.
- (36) Buterbaugh, J. S.; Toscano, J. P.; Weaver, W. L.; Gord, J. R.; Hadad, C. M.; Gustafson, T. L.; Platz, M. S. *J. Am. Chem. Soc.* **1997**, 119, 3580.
- (37) Demas, J. N.; Crosby, G. A. *J. Phys. Chem.* **1971**, 75, 991.
- (38) Knutson, J. R.; Beechem, J. M.; Brand, L. *Chem. Phys. Lett.* **1983**, 102, 501.
- (39) Beechem, J. M.; Ameloot, M.; Brand, L. *Chem. Phys. Lett.* **1985**, 120, 466.
- (40) van Stokkum, I. H. M. *IEEE Trans. Instr. Meas.* **1997**, 46, 764.
- (41) Press, W. H.; Flannery, B. P.; Teukolsky, S. A.; Vetterling, W. T. *Numerical Recipes—The Art of Scientific Computing*; Cambridge University Press: New York, 1986.
- (42) Nikogosyan, D. N.; Oraevsky, A. A.; Rupasov, V. I. *Chem. Phys.* **1983**, 77, 131.
- (43) Crowell, R. A.; Bartels, D. M. *J. Phys. Chem.* **1996**, 100, 17 940.
- (44) Calderbank, A.; Charlton, D. F.; Farrington, J. A.; James, R. J. *Chem. Soc., Perkin I* **1972**, 138.
- (45) Mau, A. W.-H.; Overbeek, J. M.; Loder, J. W.; Sasse, W. H. F. *J. Chem. Soc., Faraday Trans. 2* **1986**, 82, 869.
- (46) Birks, J. B. *Photophysics of Aromatic Molecules*; Wiley-Interscience: New York, 1970.
- (47) Novakovic, V.; Hoffman, M. Z. *J. Am. Chem. Soc.* **1987**, 109, 2341.
- (48) Kuczynski, J. P.; Milosavljevic, B. H.; Lappin, A. G.; Thomas, J. K. *Chem. Phys. Lett.* **1984**, 104, 149.
- (49) Villemure, G.; Detellier, C.; Szabo, A. G. *J. Am. Chem. Soc.* **1986**, 108, 4658.
- (50) Novakovic and Hoffman wrote in ref 47 that there is “no evidence for bona fide luminescence from  $MV^{2+}$ .”
- (51) Kosower, E. M.; Cotter, J. L. *J. Am. Chem. Soc.* **1964**, 86, 5524.
- (52) Miller, L. L.; Nordblom, G. D.; Mayer, E. A. *J. Org. Chem.* **1972**, 37, 916.
- (53) S. G. Lias, “Ionization Energy Evaluation” in NIST Chemistry WebBook, NIST Standard Reference Database Number 69, Eds. W. G. Mallard and P. J. Linstrom, February 2000, National Institute of Standards and Technology, Gaithersburg MD, 20899 (<http://webbook.nist.gov>).
- (54) Cassidy, J.; Kho, S. B.; Pons, S.; Fleischmann, M. *J. Phys. Chem.* **1985**, 89, 3933.
- (55) Buntinx, G.; Naskrecki, R.; Poizat, O. *J. Phys. Chem.* **1996**, 100, 19 380.
- (56) Schmulbach, C. D.; Hinckley, C. C.; Wasmund, D. *J. Am. Chem. Soc.* **1968**, 90, 6600.
- (57) This is not inconsistent with the results of Ebbesen and co-workers,<sup>30–32</sup> who described reductive quenching of  $MV^{2+*}$  by chloride ions in aqueous solution. Their solutions contained a high concentration of a chloride-containing salt to force ion association with one or more of the readily oxidized chloride counterions. In the dilute solutions studied here, no such ion pairs or ion triples exist, and the excited state of  $MV^{2+}$  deactivates before it can be quenched by diffusional encounter with chloride.
- (58) We have not included triplet states of  $MV^{2+}$  in our photophysical model because the El-Sayed rules [El-Sayed, M. A. *J. Chem. Phys.* **1962**, 36, 573; El-Sayed, M. A. *J. Chem. Phys.* **1963**, 38, 2834] predict slow intersystem crossing from a  $^1\pi-\pi^*$  state to a  $^3\pi-\pi^*$  state. In addition, little information is available about triplet states of  $MV^{2+}$ . The singlet–triplet splitting was reported to be 3.1 eV by Hopkins et al.<sup>23</sup> The triplet state energy of  $MV^{2+}(Br^-)_2$  was estimated to be 3.0 eV from the phosphorescence spectrum recorded at 77 K in an ethanol glass [Brown, N. M. D.; Cowley, D. J.; Hashmi, M. *J. Chem. Soc., Perkin II* **1979**, 462]. These values indicate that the emission seen in acetonitrile cannot be phosphorescence.
- (59) Mariano, P. S. *Acc. Chem. Res.* **1983**, 16, 130.

- (60) Venturi, M.; Mulazzani, Q. G.; Hoffman, M. Z. *Radiat. Phys. Chem.* **1984**, 23, 229.
- (61) Takamuku, T.; Tabata, M.; Yamaguchi, A.; Nishimoto, J.; Kumamoto, M.; Wakita, H.; Yamaguchi, T. *J. Phys. Chem. B* **1998**, 102, 8880.
- (62) Chachisvillis, M.; Zewail, A. H. *J. Phys. Chem. A* **1999**, 103, 7408.
- (63) Peon, J.; Kohler, B., manuscript in preparation.
- (64) Bagchi, B.; Gayathri, N. *Adv. Chem. Phys.* **1999**, 107, 1.
- (65) Peon, J.; Hoerner, J. D.; Huchton, K. M.; Xia, C.; Kohler, B., manuscript in preparation.
- (66) Bertolotti, S. G.; Cosa, J. J.; Gsponer, H. E.; Previtali, C. M. *Can. J. Chem.* **1987**, 65, 2425.
- (67) Szwarc, M. *Acc. Chem. Res.* **1969**, 2, 87.
- (68) Fleischmann, M.; Pletcher, D. *Tetrahedron Lett.* **1968**, 60, 6255.
- (69) Gutsev, G. L. *J. Chem. Phys.* **1993**, 98, 444.
- (70) Gutsev, G. L.; Jena, P.; Bartlett, R. J. *Chem. Phys. Lett.* **1998**, 292, 289.
- (71) Gutsev, G. L.; Boldyrev, A. I. *Chem. Phys.* **1981**, 56, 277.
- (72) Wang, X. B.; Ding, C. F.; Wang, L. S.; Boldyrev, A. I.; Simons, J. *J. Chem. Phys.* **1999**, 110, 4763.
- (73) Sowada, U.; Holroyd, R. A. *J. Chem. Phys.* **1979**, 70, 3586.
- (74) Sowada, U.; Holroyd, R. A. *J. Phys. Chem.* **1981**, 85, 541.
- (75) Born, M. Z. *Physik* **1920**, 1, 45.
- (76) Product analysis following UV irradiation of methyl viologen provides further evidence that oxidation of methanol takes place.<sup>23</sup> Ledwith et al. were able to trap the methoxy radical using a nitron spin trap and demonstrate that this species is an intermediate in the photoreduction mechanism [Ledwith, A.; Russell, P. J.; Sutcliffe, L. H. *Proc. R. Soc. London A* **1973**, 332, 151]. Our results show for the first time that electron donation by methanol occurs on an ultrafast time scale.
- (77) Kandori, H.; Kemnitz, K.; Yoshihara, K. *J. Phys. Chem.* **1992**, 96, 8042.
- (78) Yoshihara, K.; Yartsev, A.; Nagasawa, Y.; Kandori, H.; Douhal, A.; Kemnitz, K. *Pure Appl. Chem.* **1993**, 65, 1671.
- (79) Yoshihara, K. *Adv. Chem. Phys.* **1999**, 107 Pt. 2, 371.